
Patch augmentation: Towards efficient decision boundaries for neural networks

Marcus D. Bloice · Andreas Holzinger

Abstract In this paper we propose a new augmentation technique, called *patch augmentation*, that, in our experiments, improves model accuracy and makes networks more robust to adversarial attacks. In brief, this data-independent approach creates new image data based on image/label pairs, where a patch from one of the two images in the pair is superimposed on to the other image, creating a new augmented sample. The new image’s label is a linear combination of the image pair’s corresponding labels. Initial experiments show a several percentage point increase in accuracy on CIFAR-10, from a baseline of 80.6% to 86.8%. CIFAR-100 sees better improvements still. Networks trained using patch augmentation are also more robust to adversarial attacks, which we demonstrate using the Fast Gradient Sign Method.

An adversarial misclassification, or adversarial attack, occurs when an image that should seemingly be easily classified correctly by the network is suddenly classified as belonging to a completely different class—and with high confidence. Such occurrences are difficult to diagnose and are a cause of much concern in artificial intelligence research, as any model trained with empirical risk minimisation seems to be vulnerable to such attacks. The ease at which neural networks are susceptible to adversarial perturbations are partially the result of images lying close to the decision boundaries that are typically learned by neural networks during their training. Patch augmentation is an attempt to train more efficient decision boundaries.

Keywords Augmentation · Adversarial attacks · Decision boundaries

1 Introduction

A recent article in *Nature* has reported on the concerns within artificial intelligence research at the ease at which neural networks are “fooled” by adversarial examples [7]. In other words, it has increasingly been shown that state-of-the-art

Marcus D. Bloice · Andreas Holzinger
Institute for Medical Informatics, Statistics, and Documentation, Medical University Graz,
Austria
E-mail: marcus.bloice@medunigraz.at

neural networks are failing in quite unexpected and often catastrophic ways. An adversarial example is data, for example an image, that contains an almost imperceptible alteration to it, which when fed in to a neural network causes it to misclassify the image in unpredictable ways, often with a high degree of confidence. This is believed to be at least partially caused by the decision boundaries that are typically learned by neural networks in combination with empirical risk minimisation.

An early mention of adversarial examples was in 2014 by a team from Google [14]. They used the term “adversarial examples” for the images that were able to “trick” well performing neural networks, seemingly with ease. This led to concerns that neural networks were perhaps brittle or fragile, and that despite counter measures such as regularisation, networks were in fact memorising data sets too closely. The fragility of neural networks to adversarial attacks is perhaps most clearly illustrated by work performed in [13] that showed networks can output a confident, incorrect prediction by altering just a single pixel in an input image. The real life seriousness of adversarial examples was demonstrated nicely by [3], where the authors showed road signs that to the human eye clearly showed a speed limit or stop sign, but was interpreted by a neural network as something quite dangerous, such as a much higher speed limit.

Neural networks and deep learning are increasingly being used in medicine, particularly in the field of digital pathology where AI is seen as a potentially lucrative area where highly skilled pathologists could be supported by deep learning-based systems. However, a study in the journal *Science* has shown that cancer misdiagnosis can occur due to tiny adversarial perturbations, in networks that perform extremely well under normal circumstances [4]. More worrying still is the work of [14] that has shown that adversarial examples can be transferred across different networks, trained with different hyper-parameters, such as the number of layers, trained on different subsets of the same dataset, and still be susceptible to the same adversarial attacks across all these trained models. In other words, one does not need access to the trained network in order to devise an adversarial attack.

Adversarial examples are not limited to neural networks, however. It has been shown that several types of algorithm are susceptible to adversarial misclassifications [12]). It has been shown that multi-class Logistic Regression, Support Vector Machines, Decision Trees, and k -Nearest Neighbours are all susceptible to exactly the same types of attacks or examples. This is likely due to an inherent weakness issue with training any algorithm with empirical risks minimisation.

Networks where images lie close to their learned decision boundaries are considered to be partially responsible for these errors [5]. Attempts are afoot to regularise training so that more efficient decision boundaries can be learned. We believe one such approach could be through proper data augmentation, and in this work we describe an approach that attempts to coerce networks into making less confident decisions, and hence be less prone to misclassification due to adversarial perturbations. Therefore, in this paper we propose an augmentation technique to counter the issues that result in unfavourable decision boundaries. Primarily, this to alleviate the issue of adversarial attacks and misclassifications, however the technique is also useful to mitigate against memorisation and can make networks more general. We demonstrate here our method, called *patch augmentation*, and provide empirical evidence of its performance. This is done both by showing its improved accuracy on a number of standard data sets compared to a baseline accuracy,

and through the use of software designed to test networks for their robustness to adversarial attacks.

1.1 How Patch Augmentation Works

In essence, patch augmentation works by creating new image data based on pairs of images and their labels. As Figure 1 shows, a patch of a certain size is copied from image A and superimposed on to image B at a random location, creating a new augmented image, C. The new image's label, which needs to be one-hot-encoded, is also adjusted taking into account the size of the patch's area compared to the entire image. See Section 3 for more specific details on the algorithm's implementation.

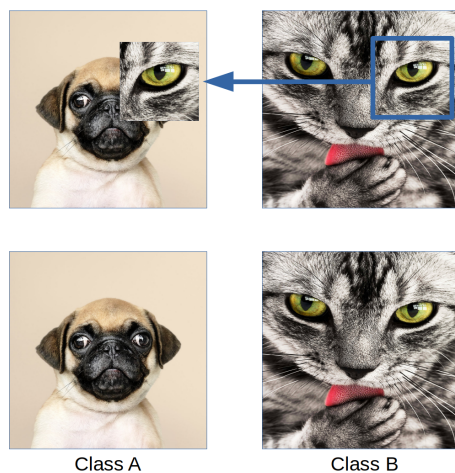


Fig. 1 The simplest form of patch placement, where a patch from *Class B* is placed in to *Class A* without alteration to the patch or to its location. In this example, the patch is placed at the same position from which it was taken and is of the same size, however as it is implemented and for the experiments in this paper, the patch's location was always placed in a random location. This creates a new image, shown on the top left of the figure above. Its new label, which must be one hot encoded, is computed from the original pair's two labels, in this case the computed label is $\tilde{y} = [0.85 \ 0.15]$, as the patch's area is 15% of the new image's size and the original image pair's labels are $y_a = [1.0 \ 0.0]$ and $y_b = [0.0 \ 1.0]$ for Class A and Class B respectively.

Source code, Jupyter demonstration notebooks, and the complete experimental setup for the patch augmentation method described in this paper can be found here under:

<https://github.com/mbloice/Patch-Augmentation>

In the next section we discuss related work in the field of image augmentation, then a more complete description of patch augmentation follows with some illustrative examples and finally the empirical results are presented.

2 Related Work

In essence, image augmentation is a technique used to regularise networks and make them more general. The procedure involves expanding an existing data set by applying transformations to the training image data in order to create new data, while ensuring that the data’s labels are preserved. Increasing the size of a data set in this way can prevent memorisation of the data set, and hence prevent overfitting. Image augmentation in the field of machine learning was performed as far back as LeCun in 1998 [10], where random distortions were applied to the original MNIST images to create new samples. The distortions that can be applied to images range from simple rotations or flips along the horizontal and vertical axes, to more advanced methods, such as elastic distortions. Indeed, the wide breadth of different types of augmentation has led to the development of augmentation libraries, such as *Augmentor*¹, written by the first author of this paper [1].

However, image augmentation is generally a data-dependent task that requires a certain amount of domain knowledge in order to develop a successful augmentation strategy. For example, it must be clear that any transformations that are applied to the image data are label preserving—for instance, that a horizontal flip will not result in an image where its label is no longer representative of the image’s contents. A simple example might be the figure 8 in a digit recognition task. The figure 8 can be translated through both the horizontal and vertical axes while preserving the image’s label, while the figure 7 cannot be translated through either axis without its label no longer representing the image—an upside 7 simply doesn’t make sense. In other words, the augmentation strategy that is used requires domain knowledge.

Approaches to create data-independent augmentation techniques include AutoAugment [2] where the augmentation procedure is learned as the network is trained, adjusting the augmentation policy’s hyper-parameters on the fly. However, this procedure adds a further learning procedure, which requires more training time and iterations. Work by [16] demonstrated the *mixup* algorithm which performs a linear combination of two images and their (one-hot encoded) labels to create augmented images. This approach proved to be highly effective, and in this work we wish to propose a similar, more parametric technique which outperforms mixup in our experiments. More recently than AutoAugment, a population-based automatic augmentation technique has been proposed [8] which performs more efficiently than AutoAugment.

Therefore, in this work, we discuss patch augmentation, which is a data-independent approach aimed at improving model generalisation and mitigating against adversarial attacks. In the next section we describe our approach in detail before moving on to empirical results.

3 Implementation and Algorithm

As briefly described in Section 1.1, patch augmentation functions by gathering pairs of images and labels, and superimposing a patch from one image on to the other image, creating a new augmented image. This is demonstrated clearly in

¹ See <https://github.com/mdbloice/Augmentor>

Figure 1. As Figure 1 shows, the new image contains a cross between the two classes, in this case that of a cat and a dog, with the dog comprising 85% of new image's area, and the cat comprising 15% of the new image's area. Because of this, the new image's label is created through a linear combination of the original pair's labels (see also the method in [16]). In the case of the example shown in Figure 1 this new label, \tilde{y} , is $[0.85, 0.15]$ as it contains a patch which has an area 15% of the size of the overall image.

Concretely, for a given augmented training image, the new image's label is calculated as follows (we will use the notation described in [16] for consistency):

$$\tilde{y} = (1 - \lambda)y_i + \lambda y_j$$

The value for λ is calculated as follows:

$$\lambda = \frac{|x_p|}{|x_i|}$$

where $|x_p|$ and $|x_i|$ denote the area in pixels of the patch, x_p , and the area in pixels of the image, x_i , respectively.

It follows, therefore, that:

$$\tilde{y} = \left(1 - \frac{|x_p|}{|x_i|}\right)y_i + \frac{|x_p|}{|x_i|}y_j$$

For example, a patch of size 200×200 placed within an image of size 400×400 would result in:

$$\lambda = \frac{|x_p|}{|x_i|} = \frac{200 \cdot 200}{400 \cdot 400} = \frac{40000}{160000} = 0.25$$

Hence:

$$\begin{aligned}\tilde{y} &= (1 - 0.25) \times [1.0 \ 0.0] + 0.25 \times [0.0 \ 1.0] \\ \tilde{y} &= 0.75 \times [1.0 \ 0.0] + 0.25 \times [0.0 \ 1.0] \\ \tilde{y} &= [0.75 \ 0.0] + [0.0 \ 0.25] \\ \tilde{y} &= [0.75 \ 0.25]\end{aligned}$$

New labels are generated for each newly created, augmented image. It is a requirement for patch augmentation that the labels are one hot encoded.

While the entire source code for patch augmentation can be found on GitHub, under the URL shown in Section 1.1, Listing 1 shows the algorithm's main functionality. The GitHub repository also contains more technical documentation of its implementation within the Keras framework, and contains Jupyter notebooks so that the experiments described here can be fully reproduced.

As can be seen in Listing 1, every image within a batch that is about to be passed to the network during training is augmented with a patch according to a user-defined probability. If this probability is set to 0, no images are altered, and the network trains with the dataset untouched. If this is set to 1 then every image within every batch is altered with a randomly placed patch. If an image is augmented, this replaces the image in the batch with the augmented sample and the same applies to its corresponding new label. Once every image in the batch is

cycled through, it is passed to the network for training. The procedure is written as a Python generator, which is used by Keras to train the network. By following the code in Listing 1, it can be seen that patches are being drawn from the entire training set. This means patches could be drawn from images of the same class, or even, although highly unlikely, the same image. When drawing only from other classes, the accuracy of the trained network was approximately equal, and had little impact on accuracy. While the patches are taken from random coordinates, they are placed at the same coordinates in the augmented image from which the patch was extracted.

```

1  for i in range(len(batch_x)):
2
3      # Perform according to user-defined probability
4      if np.random.uniform(0, 1) <= probability:
5
6          # Choose a random image from the training set
7          r_i = np.random.randint(0, len(x_train))
8
9          # Calculate random patch location
10         x1 = np.random.randint(0, dim - crop_dim)
11         x2 = x1 + crop_dim
12         y1 = np.random.randint(0, dim - crop_dim)
13         y2 = y1 + crop_dim
14
15         # Place patch to create new image data
16         batch_x[i][x1:x2,y1:y2,:] = x_train[r_i][x1:x2,y1:y2,:]
17
18         lambda_value = patch_area
19
20         # Create new label for augmented image
21         batch_y[i] = (1 - lambda_value) * batch_y[i]
22                     + lambda_value * y_train[r_i]
23
24     return batch_x, batch_y

```

Listing 1 Patch augmentation basic algorithm.

Last, it is important to note that there are two main parameters that can be adjusted: the *probability* and the *patch area*. The probability adjusts how many of the images are augmented—a value of 0.5 means half of the images during an epoch are augmented with patches. The patch area controls the size of the patches applied to the images, with 1.0 meaning the entire image is superimposed with a patch of the same size as the image, and 0 meaning no patch is applied as its size is zero pixels. Unless otherwise stated, the results reported here use a probability of 0.5 and a patch area of 0.25.

4 Experiments

Our hardware setup was a single workstation utilising a Titan X GPU running on Ubuntu 18.04. We compared various patch augmentation hyper-parameters and configurations using the CIFAR-10 and CIFAR-100 data sets and the ResNet v1 and v2 architectures. CIFAR-10 comprises 60,000 32×32 pixel images across 10 classes, equally distributed. 50,000 images are used for training and 10,000 are used for testing. CIFAR-100 is identical except that it consists of 100 classes

with 600 images each [9]. The ResNet networks were chosen as they are not very computationally demanding, and their saved model sizes are comparatively small.

For this work two main parameters were tuned—namely the patch’s area and the probability that an image is augmented with a patch. However, unless otherwise stated, the probability was set to 0.5 and the patch area was set to 0.25.

Each data set is handled in the following sub-sections. The code used to produce these results, using a random number generator seed, can be found on the paper’s GitHub repository. The Jupyter notebooks contained there are entirely self contained and can be used to replicate the experiments, results, and all plots contained in this paper.

4.1 CIFAR-10

The ResNet20v1 network performance was measured at 80.86% as a baseline (see Figure 2 for accuracy and Figure 3 for loss), and 86.83% using a network trained with patch augmentation (see Figure 4 for accuracy and Figure 5 for loss), an improvement of over 5%.

ResNet29v2 network performance was 88.01% with patch augmentation (See Figure 6 for accuracy and Figure 7 for loss) compared to 83.15% (Figure 8 for accuracy and Figure 9 for loss) for the baseline.

4.2 CIFAR-100

The baseline for CIFAR-10 using ResNet20v1 was 44.08% accuracy (see Figure 10 for accuracy and Figure 11 for loss). Using augmentation the results improved to 55.15% (See Figure 12 for accuracy and Figure 13 for loss), an improvement of over 10%. The results for the patch augmentation run were obtained using a probability of 0.5 and a patch area of 0.5, as apposed to 0.25 for the CIFAR-10 runs.

5 Robustness to Adversarial Attacks

In order to test the robustness of the networks trained with patch augmentation to adversarial attacks, we used the *CleverHans* library, developed mostly by members of Google Brain, among others [11].

CleverHans contains a number of adversarial attack creation algorithms. These attacks accept a model and a test set as input, and it returns the corresponding adversarial examples. A number of attacks are available, however we tested the trained network using the Fast Gradient Sign Method (FGSM) [6]. In this white-box attack, where access to the trained model is required to generate the attacks, the network’s gradients are used to create the adversarial example that will trick the network. For a given input image, x , FGSM uses the gradients of the loss w.r.t. the input image to create a new image, \tilde{x} , that maximises the loss [15]:

$$\tilde{x} = x + \epsilon \cdot \text{sign}(\nabla_x J(\theta, x, y))$$

where ϵ controls the magnitude of the perturbation—in our case, this was set to 0.001 and 0.03 to see the effect of the perturbation change. Larger values of ϵ means the network is more likely to misclassify \tilde{x} , however this also means that it is more detectable by a human. We benchmarked the robustness of our method to adversarial attack using v3.0.1 of CleverHans. On a test set modified by the Fast Gradient Sign Method with a max-norm ϵ of 0.001, we obtained a test set accuracy of (on the first 1,000 images in the CIFAR-10 test set) of 64.3% accuracy using the non-augmented model, versus 72.5% accuracy using the model trained with patch augmentation. When increasing ϵ to 0.03, accuracy degraded significantly, however, the network trained with patch augmentation performed better with an accuracy of 20.1% compared to 13.8% for the standard model trained without augmentation. The GitHub repository (see Section 1.1) contains a notebook where the experiments have been performed, along with the trained models in HDF5 format that were used for the generation of the adversarial examples.

6 Results Summary

Our experiments show encouraging results, with patch augmentation consistently outperforming baseline accuracy on several data set and network configurations. For CIFAR-10 using ResNet20v1 we achieved a baseline accuracy of 80.86%, which improved to 86.63% with patch augmentation. For CIFAR-10 using ResNet29v2 we achieved a baseline accuracy of 83.15% compared to 88.01% accuracy when using patch augmentation. For CIFAR-100 we achieved a baseline accuracy of 44.08%, which improved to 55.15% when using patch augmentation. When compared to mixup, patch augmentation slightly outperformed it, with mixup achieving 86.62% accuracy (see Figure 14 for accuracy and Figure 15 for loss).

Table 1 shows a summary of the results on various network and data set configurations.

Model	CIFAR-10	CIFAR-100
ResNet20v1	80.86%	44.08%
ResNet20v1 + patch	86.83%	55.15%
ResNet29v2	83.15%	-
ResNet29v2 + patch	88.01%	-

Table 1 Summary of trained model accuracies for CIFAR-10 and CIFAR-100 using ResNetv1 and ResNetv2.

Adversarial Attack	No Augmentation	Patch Augmentation
FGSM ($\epsilon = 0.001$)	64.3%	72.5%
FGSM ($\epsilon = 0.03$)	13.8%	20.1%

Table 2 Summary of trained model accuracies for FGSM generated adversarial examples (ResNet20v1/CIFAR-10)

As for adversarial attacks, patch augmentation proved to be more robust to adversarial perturbations compared to a network trained without augmentation. The network trained with patch augmentation classified 72.5% of the adversarial images correctly, compared to 64.3% for a model trained without augmentation, as summarised in Table 2. Adjusting ϵ reduces accuracy dramatically, as expected. However, the network trained with patch augmentation still outperforms the network trained without augmentation, showing that it is more robust to adversarial examples generated with larger values of ϵ also.

7 Conclusions

Data augmentation is an important part of deep learning, and is used almost by default for any neural network based model learning. It is used to train more general models, avoid over-fitting, and avoid memorisation. In this paper we have provided a data-independent approach that increases classification accuracy in a number of scenarios, but has also been shown to strengthen networks against adversarial attacks. In terms of accuracy, we have seen that patch augmentation increased the accuracy of neural networks on some common data sets when compared to baseline models without any augmentation applied. Accuracy increased by over 6% for CIFAR-10 and over 10% for CIFAR-100. As well as this, we have seen that in initial experiments, patch augmentation slightly outperforms mixup with an identical network and data set configuration. We have also seen that networks trained using patch augmentation are more robust to adversarial examples and attacks generated with the Fast Gradient Sign Method. This is of particular importance in artificial intelligence research, due to recent papers highlighting how fragile some, normally very well performing networks, seem to be.

Further work may be needed to ascertain the best parameter choices for the algorithm, or to explore the effect of augmentation on the patch data itself. Patch augmentation has the potential to be a highly parametric approach. The patches themselves can be of a fixed size, or they can be randomly sized. They can be placed randomly within the second image, they can always be centred, or they can be placed at the same location from which they are extracted (as is the case in the experiments reported here). Alternatively, the patches can be placed wholly within the host image, or allowed to overlap beyond the border of the host image (in effect being cropped out of the newly augmented image). The patch itself could have its transparency altered or augmentation could be applied to the patch before it is superimposed, such as with slight rotations or zooming. Future work will concentrate on finding optimal approaches.

The paper’s GitHub repository will be updated to contain any further experimental results, as and when they are performed. Last, the technique will be added to the Augmentor software library (maintained by the first author of this paper) as a standard feature of the package, so that patch augmentation can be applied to existing machine learning training pipelines conveniently.

Acknowledgements We are grateful to Peter M. Roth, Graz University of Technology, for discussions and comments. Images obtained from Pexels and are free to use under CC0 licence.

Conflict of interest

The authors declare that they have no conflict of interest.

References

1. Bloice, M.D., Roth, P.M., Holzinger, A.: Biomedical image augmentation using Augmentor. *Bioinformatics* **35**(1), 4522–4524 (2019)
2. Cubuk, E.D., Zoph, B., Mane, D., Vasudevan, V., Le, Q.V.: Autoaugment: Learning augmentation policies from data. [arXiv:1805.09501](https://arxiv.org/abs/1805.09501) (2018)
3. Eykholt, K., Evtimov, I., Fernandes, E., Li, B., Rahmati, A., Xiao, C., Prakash, A., Kohno, T., Song, D.: Robust physical-world attacks on deep learning visual classification. In: *Proceedings of the IEEE Conference on Computer Vision and Pattern Recognition (CVPR 2018)*, pp. 1625–1634 (2018)
4. Finlayson, S.G., Bowers, J.D., Ito, J., Zittrain, J.L., Beam, A.L., Kohane, I.S.: Adversarial attacks on medical machine learning. *Science* **363**(6433), 1287–1289 (2019)
5. Ghorbani, A., Abid, A., Zou, J.: Interpretation of neural networks is fragile. In: *Proceedings of the AAAI Conference on Artificial Intelligence*, vol. 33, pp. 3681–3688 (2019)
6. Goodfellow, I.J., Shlens, J., Szegedy, C.: Explaining and harnessing adversarial examples. [arXiv preprint arXiv:1412.6572](https://arxiv.org/abs/1412.6572) (2014)
7. Heaven, D.: Why deep-learning AIs are so easy to fool. *Nature* **574**, 163–166 (2019)
8. Ho, D., Liang, E., Stoica, I., Abbeel, P., Chen, X.: Population based augmentation: Efficient learning of augmentation policy schedules. [arXiv:1905.05393](https://arxiv.org/abs/1905.05393) (2019)
9. Krizhevsky, A.: Learning multiple layers of features from tiny images. *Tech. rep.* (2009)
10. LeCun, Y., Bottou, L., Bengio, Y., Haffner, P.: Gradient-based learning applied to document recognition. *Proceedings of the IEEE* **86**(11), 2278–2324 (1998)
11. Papernot, N., Faghri, F., Carlini, N., Goodfellow, I., Feinman, R., Kurakin, A., Xie, C., Sharma, Y., Brown, T., Roy, A., Matyasko, A., Behzadan, V., Hambardzumyan, K., Zhang, Z., Juang, Y.L., Li, Z., Sheatsley, R., Garg, A., Uesato, J., Gierke, W., Dong, Y., Berthelot, D., Hendricks, P., Rauber, J., Long, R.: Technical report on the cleverhans v2.1.0 adversarial examples library. [arXiv preprint arXiv:1610.00768](https://arxiv.org/abs/1610.00768) (2018)
12. Papernot, N., McDaniel, P., Goodfellow, I.: Transferability in machine learning: from phenomena to black-box attacks using adversarial samples. [arXiv:1605.07277](https://arxiv.org/abs/1605.07277) (2016)
13. Su, J., Vargas, D.V., Sakurai, K.: One pixel attack for fooling deep neural networks. *IEEE Transactions on Evolutionary Computation* (2019)
14. Szegedy, C., Zaremba, W., Sutskever, I., Bruna, J., Erhan, D., Goodfellow, I., Fergus, R.: Intriguing properties of neural networks. [arXiv:1312.6199](https://arxiv.org/abs/1312.6199) (2013)
15. TensorFlow Documentation: Adversarial example using FGSM. https://www.tensorflow.org/tutorials/generative/adversarial_fgsm. Accessed: 2019-11-05
16. Zhang, H., Cisse, M., Dauphin, Y.N., Lopez-Paz, D.: mixup: Beyond empirical risk minimization. [arXiv:1710.09412](https://arxiv.org/abs/1710.09412) (2017)

Appendix

Plots relating to network performance are placed here.

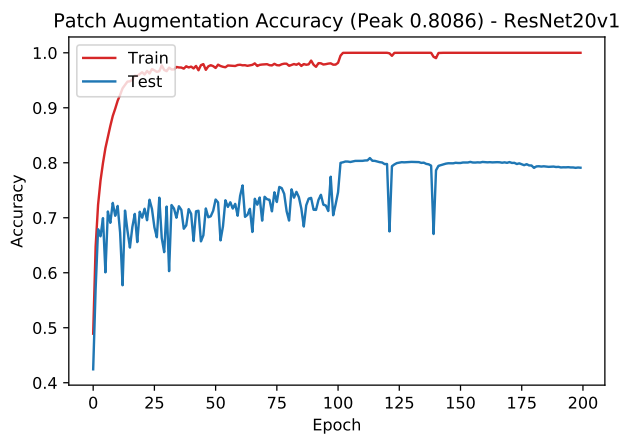


Fig. 2 Baseline accuracy on CIFAR-10 data set using ResNet20v1, over 200 epochs.

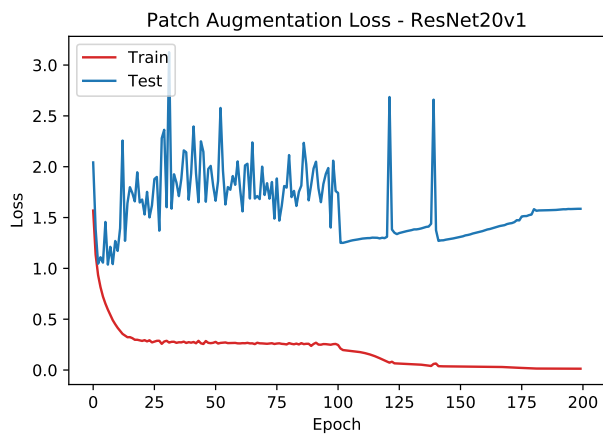


Fig. 3 Baseline loss on CIFAR-10 data set using ResNet20v1, over 200 epochs.

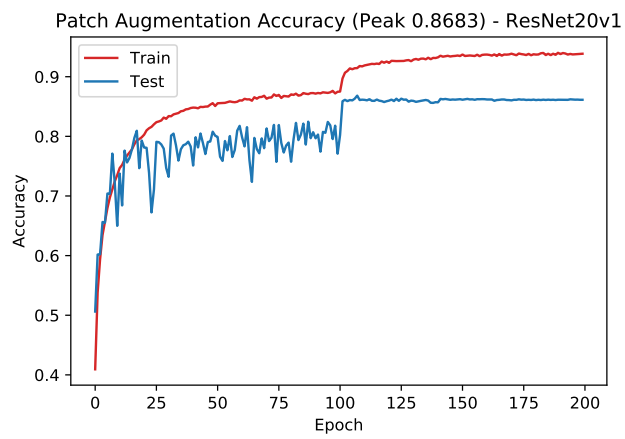


Fig. 4 Patch augmentation accuracy on CIFAR-10 data set using ResNet20v1, over 200 epochs.

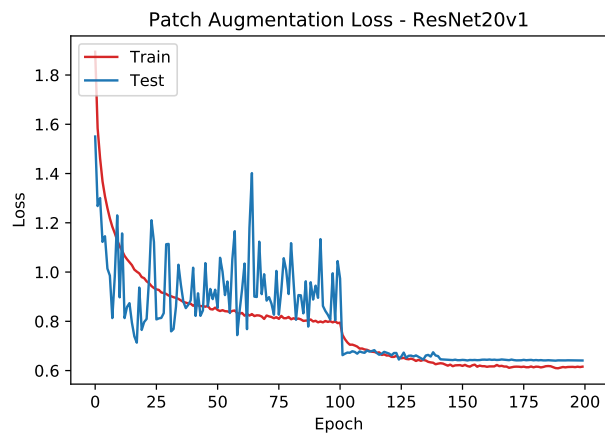


Fig. 5 Patch augmentation loss on CIFAR-10 data set using ResNet20v1, over 200 epochs.

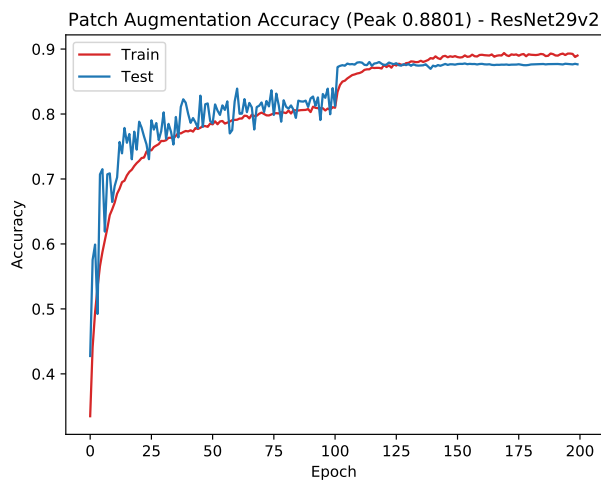


Fig. 6 Patch augmentation accuracy on CIFAR-10 data set using ResNet29v2, over 200 epochs. This is an improvement of almost 5% over the baseline for ResNet29v2 shown in Figure 8

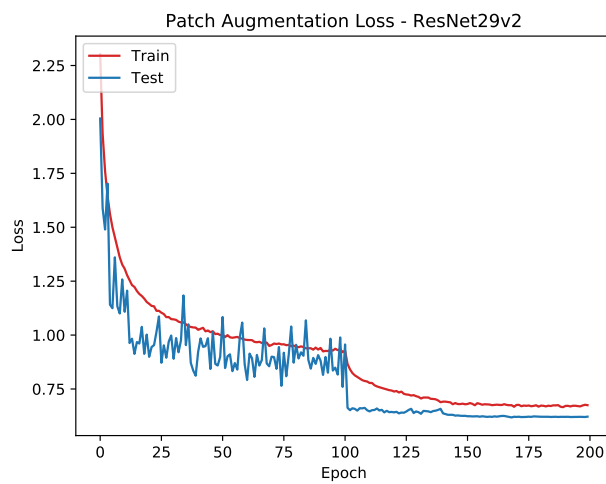


Fig. 7 Patch augmentation loss on CIFAR-10 data set using ResNet29v2, over 200 epochs.

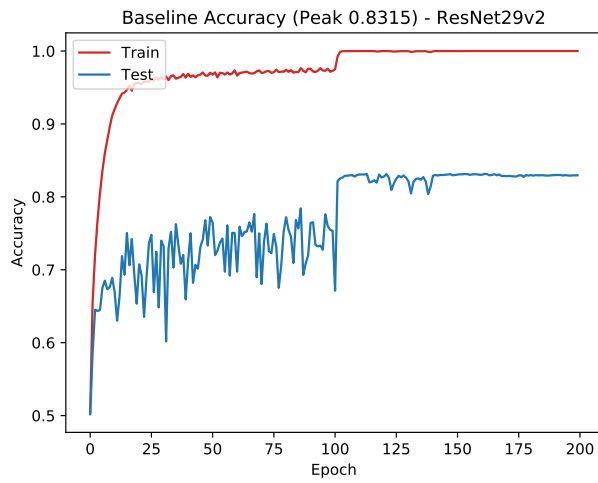


Fig. 8 Baseline accuracy on CIFAR-10 data set using ResNet29v2, with no augmentation over 200 epochs.

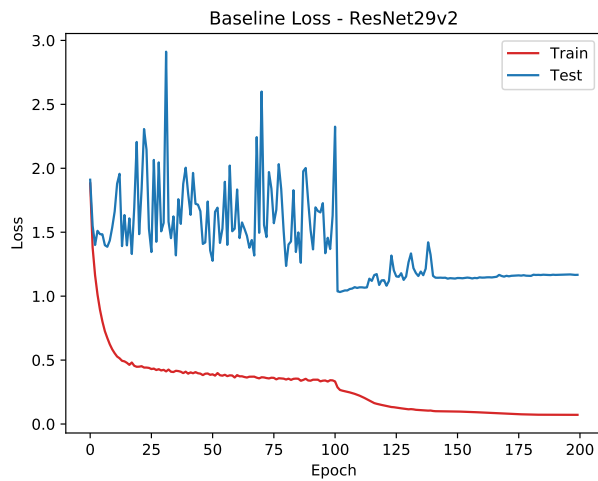


Fig. 9 Baseline loss on CIFAR-10 data set using ResNet29v2, with no augmentation over 200 epochs.

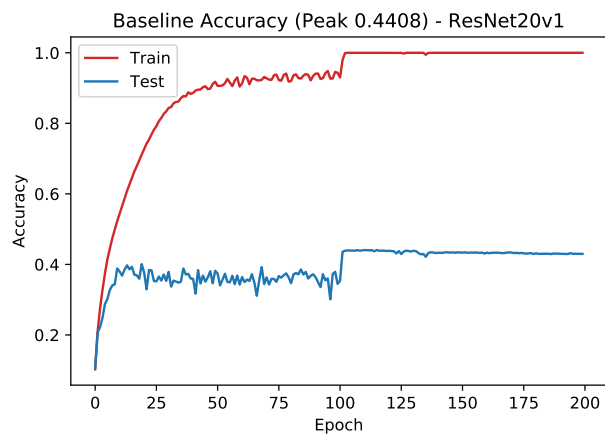


Fig. 10 Baseline accuracy on CIFAR-100 data set using ResNet20v1, no augmentation, over 200 epochs.

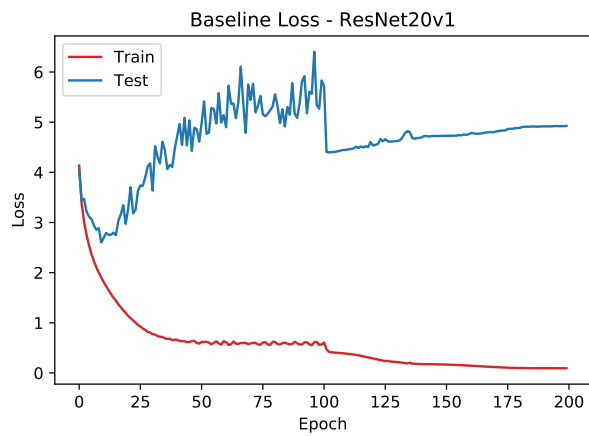


Fig. 11 Baseline loss on CIFAR-100 data set using ResNet20v1 over 200 epochs.

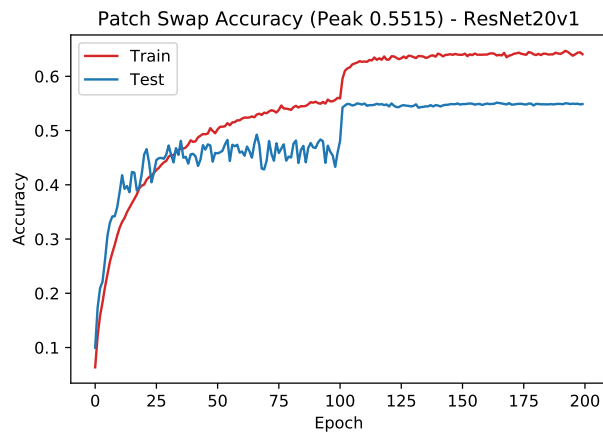


Fig. 12 Patch augmentation accuracy on CIFAR-100 data set using ResNet20v1 over 200 epochs. This is an improvement of over 10% from the baseline of 44.08% shown in Figure 10.

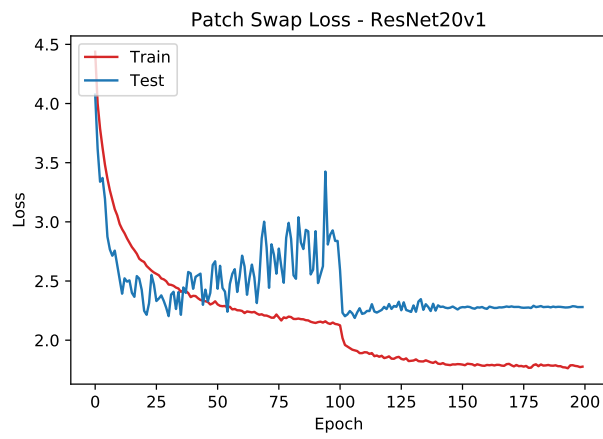


Fig. 13 Patch augmentation loss on CIFAR-100 data set using ResNet20v1 over 200 epochs.

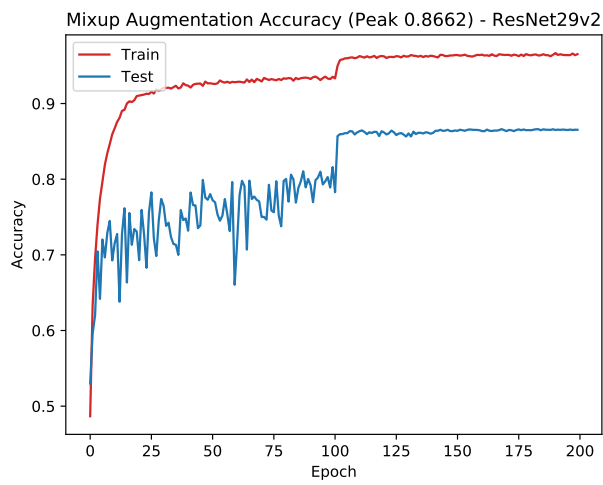


Fig. 14 Mixup augmentation accuracy values on CIFAR-10 data set using ResNet29v2, over 200 epochs. Patch augmentation slightly outperforms it, see Figure 6.

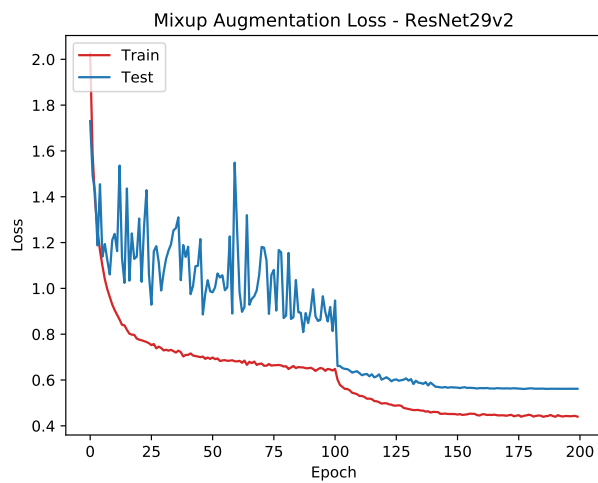


Fig. 15 Mixup augmentation loss on CIFAR-10 data set using ResNet29v2, over 200 epochs.